Hindawi
International Journal of RF and Microwave Computer-Aided Engineering
Volume 2023, Article ID 8895596, 10 pages
https://doi.org/10.1155/2023/8895596

Research Article

A Multipolarized Traveling-Wave Series-Fed Antenna Array Based on Patch

Xin Guan, Zhenghui Xue, Wu Ren, and Weiming Li

School of Integrated Circuits and Electronics, Beijing Institute of Technology, Beijing 100081, China

Correspondence should be addressed to Wu Ren; renwu@bit.edu.cn

Received 26 June 2023; Revised 25 July 2023; Accepted 10 November 2023; Published 8 December 2023

Academic Editor: N. Nasimuddin

In this paper, a simple broadband multipolarized traveling-wave series-fed antenna array is proposed. The radiation unit cells are multiple squares. The square unit cell will change between circular polarized (CP) and linear polarized (LP) through a reasonable feeding mode. By adjusting the equivalent length of the unit cell, the Q value of the antenna can be reduced, resulting in the increase of the bandwidth of the array. The array consists of seven-unit cells and dual-port feeding. The unit cells which are connected by a microstrip line are arranged in a circular array. A reasonable layout of unit cells can achieve good port isolation of the array. The polarization performance of the array antenna is the same as that of the unit cell. The antenna is fabricated and measured. The measured results are consistent with the simulated results.

1. Introduction

A multipolarized antenna plays an important role in radio communication systems because it has many advantages, such as anti-interference. Multipolarized antennas have been widely used in satellite communication systems.

The CP antenna can be achieved by introducing a single feed on the regular unit cell [1–9]. Guo and Tan proposed a wideband single-feed CP unit cell antenna [3]. The radiating elements of the antenna are two crossed printed dipoles, which incorporate a 90-phase delay line realized with a vacant-quarter printed ring [4]. The antenna can realize CP radiation. This letter presents an effective approach to design a dual-band CP slot antenna with flexible frequency ratio and similar in-band gain under the 0.5λ- and λ-mode radiation [5]. However, the bandwidth of the single-feed antenna is not wide.

In [10], a compact series-fed center-fed open-stub linear array antenna is presented. The current SR technology has been widely used in antenna design [10–12]. The array connects the units in series, which causes the sequential rotation effect [11]. In [12], a wideband CP 2×2-unit cell array is proposed, which uses a sequential-phase feeding network. These arrays are basically single-point fed. It is difficult to realize polarization conversion by single-point feeding. Thus, the multifeed will be a good choice.

There are some papers on the design of a multipolarized antenna using SR technology with two ports [1, 13–16]. An SR antenna array for millimeter wave is proposed in [13]. A dual-CP compact microstrip unit cell array is reported in [14]. This antenna is excited by a microstrip line using coplanar proximity coupling. However, the BW and ARBW of the antenna are relatively small. Using sequentially rotated feed networks, Shen et al. presented a dual-CP array in [15]. Ibrahim et al. designed an antenna consisting of some unit cells in [1]. The feed port supplies power to these unit cells with the same current and appropriate phase delay. A CP series-fed array based on the SR technique is proposed in [16–19]. The radiation elements and feed network are unified, which makes it possible to realize dual-CP radiation for series-fed SR arrays. To sum up, multipolarization of the antenna can be realized by using the SR technology and multiport feeding. A traveling-wave series-fed antenna array can increase bandwidth and realize switchable polarization.

In this paper, a novel broadband multipolarized traveling-wave series-fed antenna array is proposed. The array can be converted between RHCP, LHCP, and LP. This proposed antenna array can be used not only in radar and

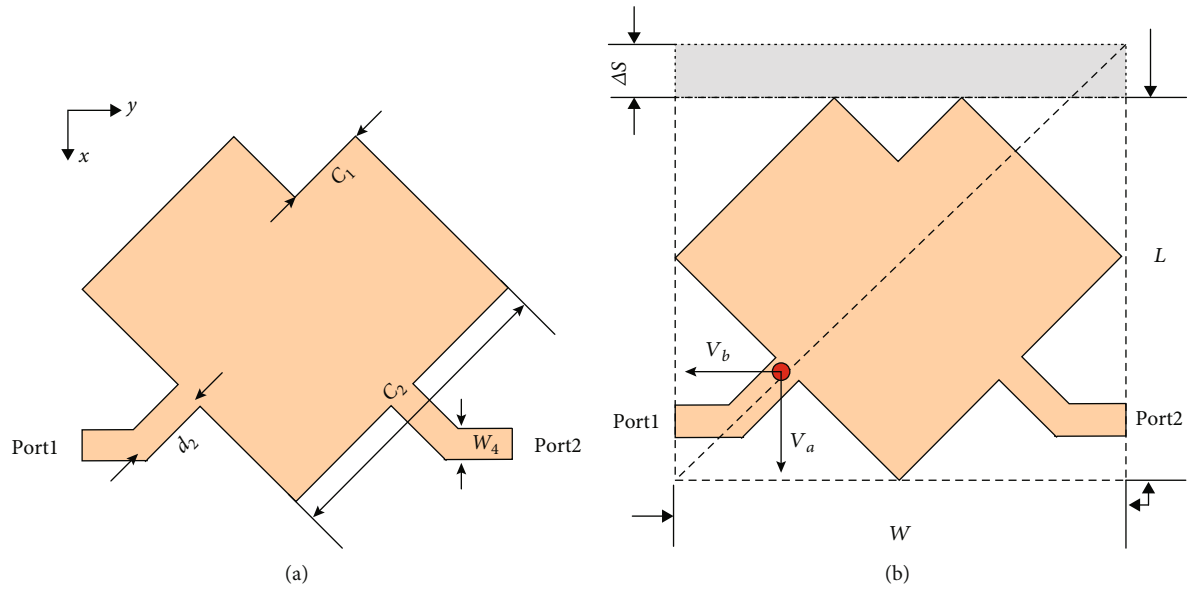

FIGURE 1: (a) Unit cell structure. The design sizes are $C_1 = 5.0$ mm, $C_2 = 17.5$ mm, $W_4 = 1.8$ mm, and $d_2 = 4.5$ mm. (b) Unit cell equivalent structure.

satellites but also in civilian vehicle speed monitoring. This letter presents a square unit cell which can realize CP and LP in the second part. By adjusting the equivalent length of the unit cell, the bandwidth of the antenna can be increased. In the third part, we connect the square unit cell end to end to form a circular array antenna. The isolation between the two ports of the antenna is high. Lastly, the fourth part introduces the measured results of the antenna, including S parameters, radiation pattern, gain, and axial ratio.

2. Unit Cell Antenna Geometry

This proposed unit cell is shown in Figure 1(a). The main structure of the unit cell is square. We take the diagonal of the unit cell as the axis, exerting the feed on the left and right sides of the unit cell. Through reasonable feeding, the unit cell can generate multiple polarized forms.

An inevitable drawback of microstrip patch antennas is their narrow bandwidth. Take the hypotenuse of the square unit cell as the side length and draw a rectangle R along its outer edge, as shown in Figure 1(b). The relationship between width W and length L is $W - L = \Delta S$. The red dot in Figure 1(b) is the feed points of rectangle R. The microstrip antenna is a circuit with a high Q value. Reducing the Q value can increase the bandwidth of the microstrip antenna. When the W/L ratio is increased, the antenna's Q value will decrease. So, we fix the value of W. The value of L will decrease as the parameter C_1 increases. When the parameter C_1 increases, the bandwidth of the microstrip unit cell increases gradually, as shown in Figure 2.

In the cavity mode theory, the arbitrary excitation mode of the microstrip antenna can be equivalent to a resonant circuit. Then, the equivalent circuit of the two modes is shown in Figure 3. The equivalent parameters of the circuit are as follows. G is the loss conductance, which is mainly determined by radiation conductance when used as an antenna. The total admittance of the two branches is, respectively, as follows:

$$Y_a = G + j(B - B_0), \tag{1a}$$

$$Y_b = G + j(B + B_0), \tag{1b}$$

where $B = \omega C - (1/\omega L)$. When formula v_a/v_b is equal to $\pm j$, the circular polarized function will be achieved.

The type of CP of the antenna can be judged according to the relationship of the phase angle leading and hysteresis. When port 1 is fed and port 2 is connected to the matching load, the formula V_a/V_b is equal to j. The unit cell can rotate clockwise to generate right-hand circular polarization (RHCP), as shown in Figure 4(a). When port 2 is fed and port 1 is connected to the matching load, the formula V_a/V_b is equal to $-j$. The unit cell will rotate counterclockwise to generate left-hand circular polarization (LHCP), as shown in Figure 4(b). A LP wave can be composed of two circular polarized waves with opposite rotations as shown in Figure 4(c). When realizing the LP of the circular array, the two ports of the antenna should be fed at the same time. During the measurement of the circular array, it is necessary to connect a power divider and phase shifter between the SMA connector and vector network analyzer. When the feed phase is adjusted, the LP at different angles can be realized.

In general, when the axis ratio of elliptical polarization is lower than 3 dB, it can be considered as CP. The LHCP wave component is perpendicular to the RHCP direction. Theoretically, the LHCP antennas cannot receive RHCP radiation waves. Therefore, it is very important that the antenna can switch between LHCP and RHCP.

In addition, the electromagnetic field of the traveling-wave antenna is set in a traveling-wave state. The reflection of the antenna is very small. The input impedance of a

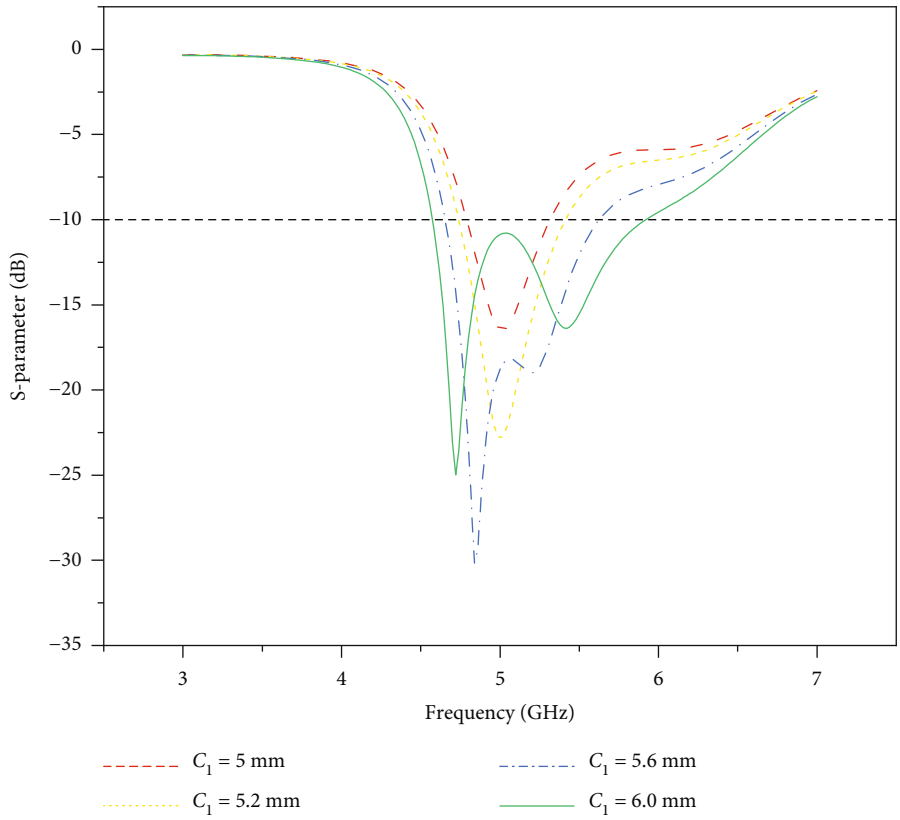

FIGURE 2: Simulated S-parameter with different C_1 of unit cell structure.

traveling-wave antenna is approximately pure resistance. Thus, the traveling-wave serial-fed antenna can improve the passband bandwidth. These unit cells are arranged in a circular array.

3. Circular Series-Fed Array

The multipolarized array can be designed with these unit cells. The circular series-fed array structure is shown in Figure 5(a). The antenna array is composed of seven-unit cells, two feed ports, and one ground. The included angle between the patches is 45 degrees. The unit cells are connected by a microstrip line. The array antenna is designed on the F4B board with a dielectric constant of 2.65 and a thickness of 1.5 mm. The simulated absolute current strength colormap for the array is shown in Figure 5(b). The simulated 3D radiation pattern plot at 5.3 GHz is shown in Figure 5(c). The FTBR of this antenna array is 19.4 dB.

Assume that the number of unit cells of the array is n, p_n represents its radiation power, and p_t represents the power transmitted along the transmission string feed array. Each unit cell can radiate different energy. The radiation power of the unit cell is related to the S parameter. The details are as follows [11].

$$P \propto \frac{1 - |S_{11}|^2 - |S_{21}|^2}{1 - |S_{11}|^2}, \tag{2}$$

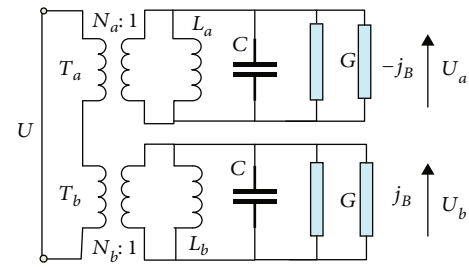

FIGURE 3: Equivalent resonant circuit of unit cell antenna.

where $|S_{11}|$ is the reflection coefficient of each element and $|S_{21}|$ is the transmission coefficient of each element.

Regardless of the various losses of the circuit, when $|S_{11}|$ is small enough, formula (2) can be rewritten as $P = 1 - |S_{21}|^2$. Therefore, we can infer that for the first unit cell, $P_1 = 1 - |S_{21}|^2$; for the second unit cell, $P_2 = (1 - P_1)P_1$; for the third unit cell, $P = (1 - P_1 - P_2)P_1 = (1 - P_1)^2 P_1$; and the radiation power of the nth unit cell is $P_n = (1 - P_1)^{n-1} P_1$. The radiation power of the unit cell forms an equal ratio sequence, and the calculated total radiation power is $P = 1 - (1 - P_1)^n$.

When the number of antenna unit cells increases, the radiation power of the antenna increases. The transmission coefficient $|S_{21}|$ of the array is expected to decrease as the line length increases. The following factors should be taken into account when selecting the number of patches for the array antenna.

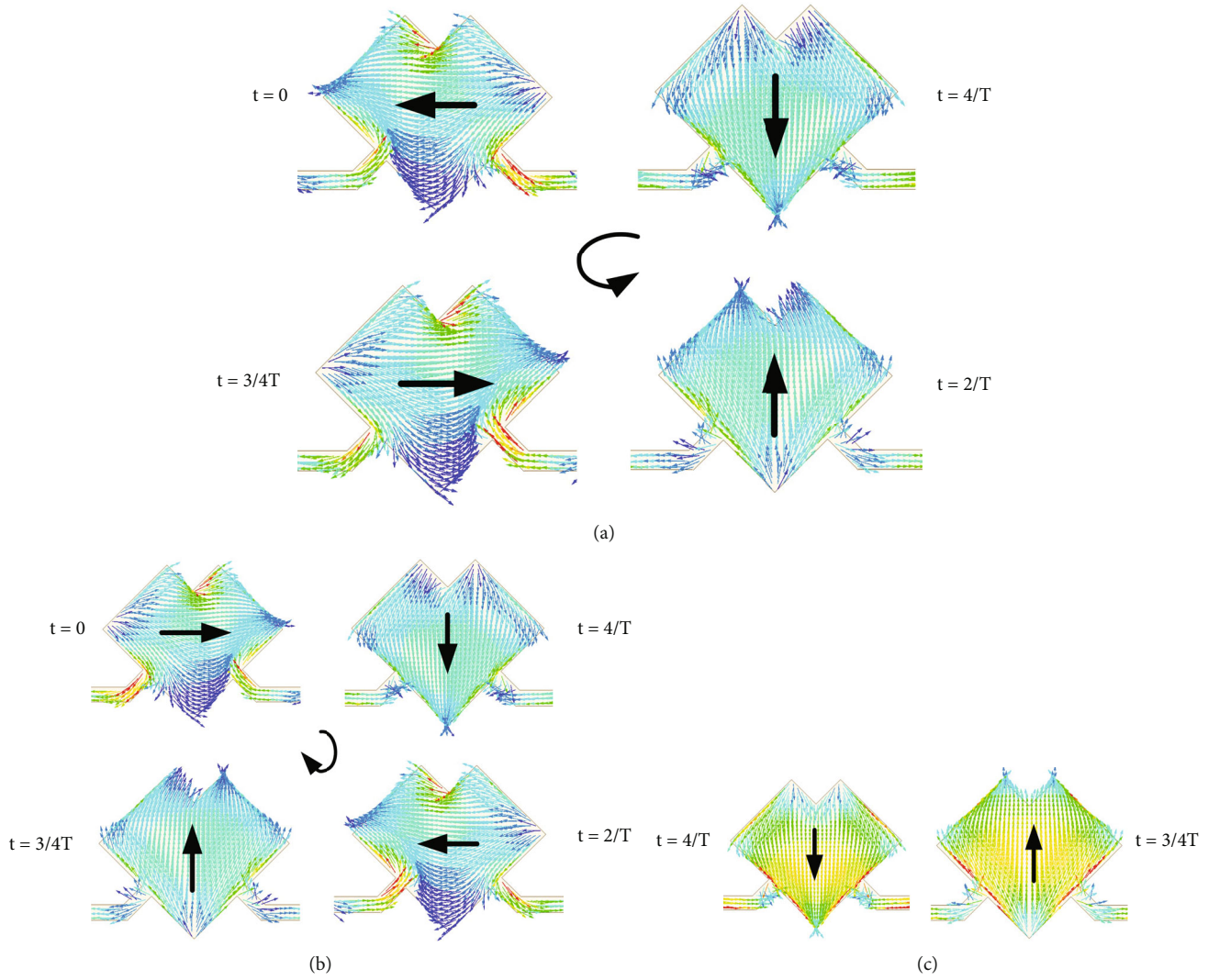

FIGURE 4: The instantaneous current distribution of unit cell fed by different polarizations. (a) Port 2 fed (RHCP); (b) port 1 fed (LHCP); (c) two ports fed (LP).

Firstly, there is a little coupling effect between the unit cells, and the distance should not be too close. Secondly, the radiation power of the antenna array should be large enough. Finally, the antenna array should be a left-and-right symmetric structure to ensure the integrity of the radiation pattern. Therefore, we select 7-unit cells to build the array.

4. Fabrication and Experimental Results

Based on the previous analysis and discussion, the circular array antenna is processed on the dielectric plate of F4B as shown in Figure 6. The *S* parameters of the array are measured by the vector network analyzer. The radiation pattern, axial ratio, and gain of the array are measured in a far-field anechoic chamber. During the measurement of the circular array, it is necessary to connect a power divider and phase shifter between the SMA connector and vector network analyzer. The phase shifter can realize different feed phases. The details are as follows.

4.1. Result of S Parameter. The *S* parameter of the antenna array can be obtained by a vector network analyzer. In Figure 7, the measured and simulated *S* parameters of this antenna array are shown. The FBW of the circular array is 17%, from 4.8 to 5.7 GHz. The bandwidth of the array antenna has been significantly improved. The array-measured reflection coefficients S_{11} are lower than −15 dB, and the transmission coefficients S_{21} are lower than −15 dB. The array has high port isolation performance, meeting the previous design requirements in the third part.

At the passband, the measured results are almost the same as the simulated results, but there are some frequency deviations. When the antenna is simulated in the software, the actual conditions such as discontinuous microstrip lines and microstrip elbows in the antenna cannot be optimized in the simulation software. Moreover, the actual machining error, SMA connector, microwave dielectric material metal loss, and dielectric loss difference also lead to frequency deviation. The microwave dielectric constant of the actual

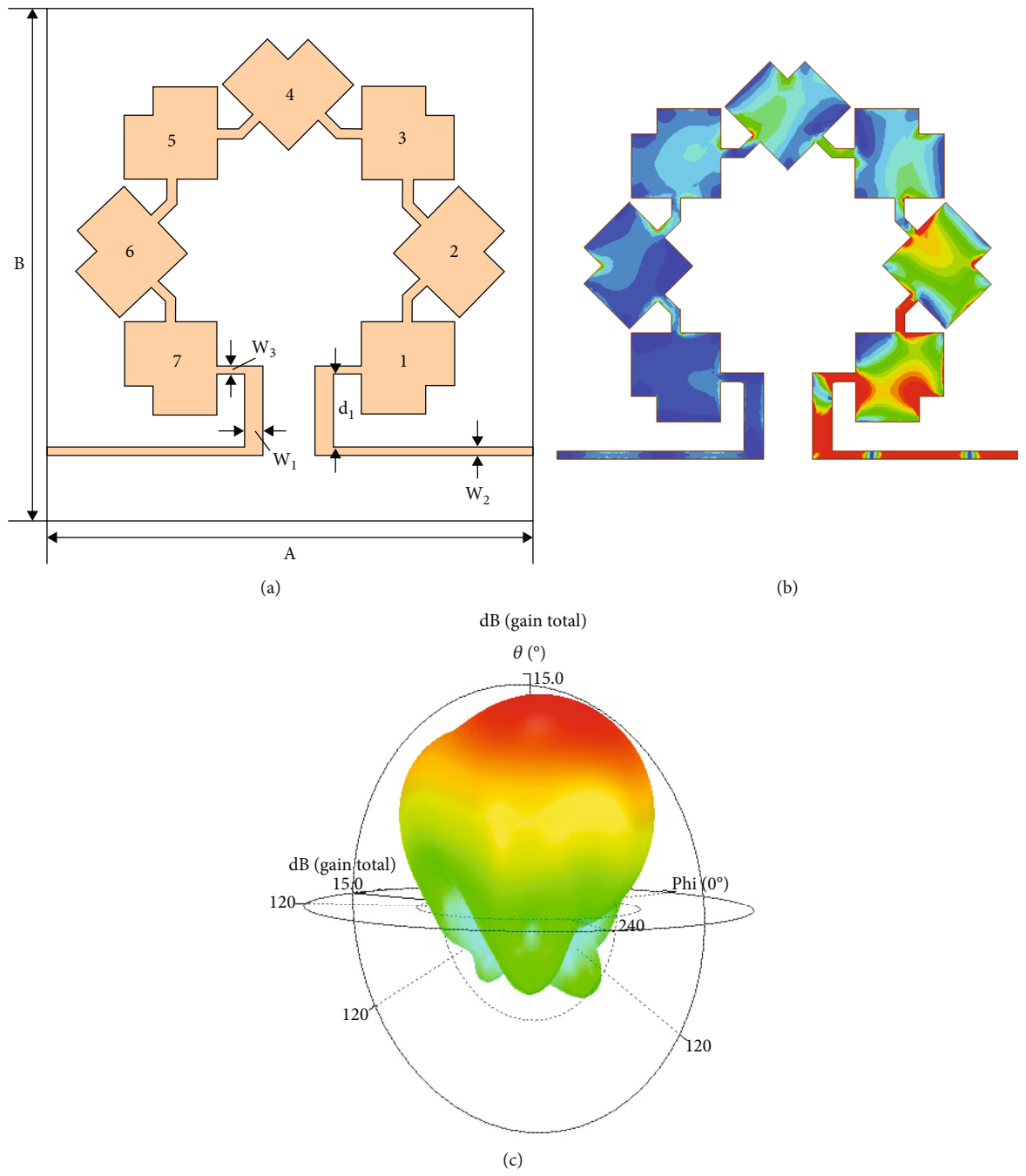

FIGURE 5: (a) The overall structure of circular array. The array design parameters are A = 90 mm, B = 95 mm, w_1 = 3.8 mm, w_2 = 1.5 mm, w_3 = 1.8 mm, and d_1 = 13.4 mm. (b) Simulated absolute current strength colormap for array. (c) Simulated 3D radiation pattern at 5.3 GHz.

processed medium plate decreases, and the frequency band will be moved up.

4.2. Result of Radiation Patterns. The measured and simulated radiation patterns in the $\varphi = 0$ deg and $\varphi = 90$ deg for RHCP and LHCP at 5.3 GHz are shown in Figure 8. Normalize the antenna pattern data. It can be seen that the simulated results of the antenna array radiation pattern are basically consistent with the measured results. The sidelobe level is mostly lower than -10 dB in the radiation pattern of the array. The difference between the main polarization and cross-polarization is about 15 dB. The measured 3 dB beamwidth is about 32° and 34° in the $\varphi = 0$ deg and $\varphi = 90$ deg of CP, respectively.

The LP array's measured and simulated 3 dB beamwidths are about 32° and 36° in the $\varphi = 0$ deg and $\varphi = 90$ deg, respectively, as shown in Figure 9. There is a little difference between the measured results and the simulated results, because during the measurement, the power divider is used to connect the port of the antenna to ensure that

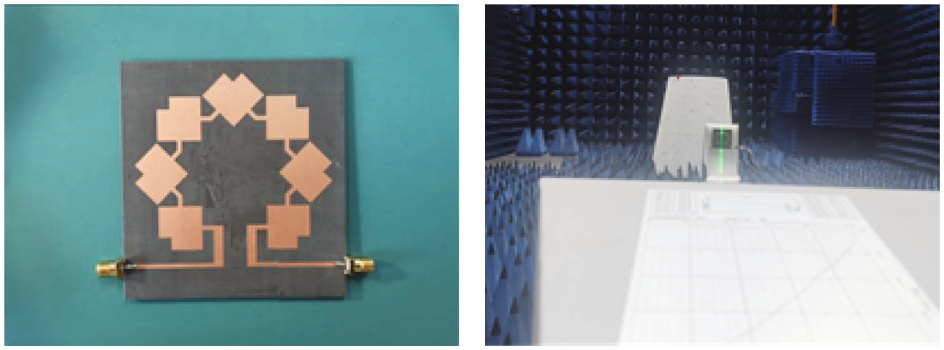

(a) (b)

FIGURE 6: (a) The photo of circular array material object; (b) photo of antenna measured in anechoic chamber.

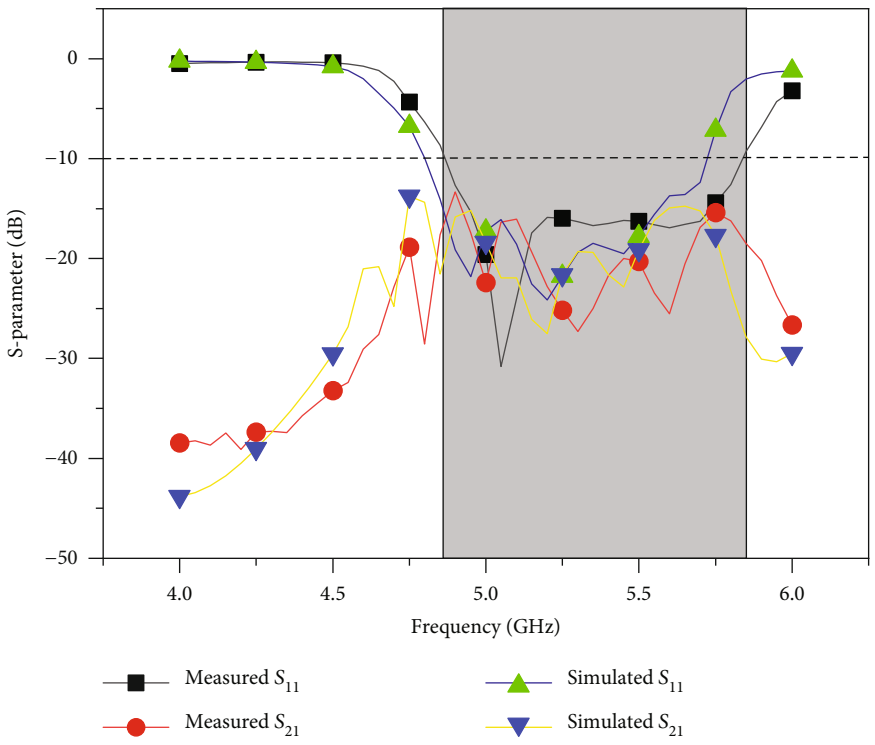

FIGURE 7: The measured and simulated *S*-parameters of this array.

the left and right ends can feed at the same time. In our future work, how to reduce the cross-polarization of linear polarization and improve the polarization purity will be the focus. We can use defected ground plane, left-handed structures and shorting wall, shorting pins, stub, and strip loadings.

4.3. Result of Axial Ratio and Gain. Generally, when the axial ratio of the antenna is less than 3, it can be considered as circular polarized radiation. In Figure 10, the simulated and measured axial ratios are shown. The ARBW of RHCP and LHCP arrays ranges from 5.0 to 5.7 GHz (13.2%). The array has good CP quality which can show that the proposed series feed array design meets the expected requirements. The simulation results are consistent with the measurement results. The BW of the array is basically consistent with the ARBW. The axial ratio of the proposed antenna meets the requirements of most circular polarization communication systems.

The simulated and measured realized broadside gains of CP and LP are shown in Figure 11. The measured CP realized gain is about 10.3 dB, and the LP realized gain is about 10 dB. The gain within the bandwidth is larger than 6 dB.

Table 1 is a comparison between our work and some existing works. Obviously, the proposed antenna array has some advantages. In Table 1, the BW of the proposed antenna is wider than that of most existing works. And the

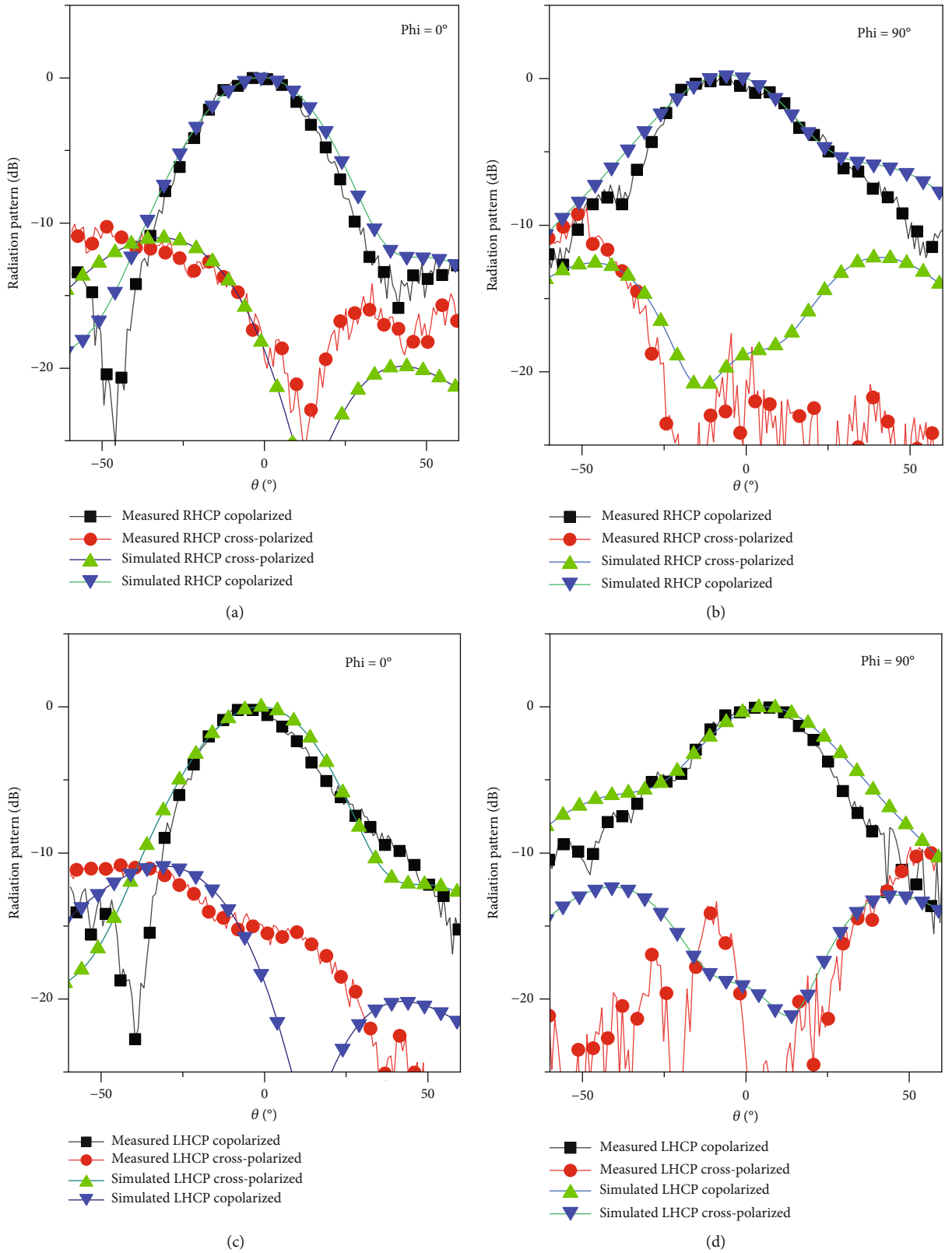

FIGURE 8: The simulated and measured radiation patterns of (a, b) RHCP and (c, d) LHCP in the $\varphi = 0$ deg and $\varphi = 90$ deg of array at 5.3 GHz.

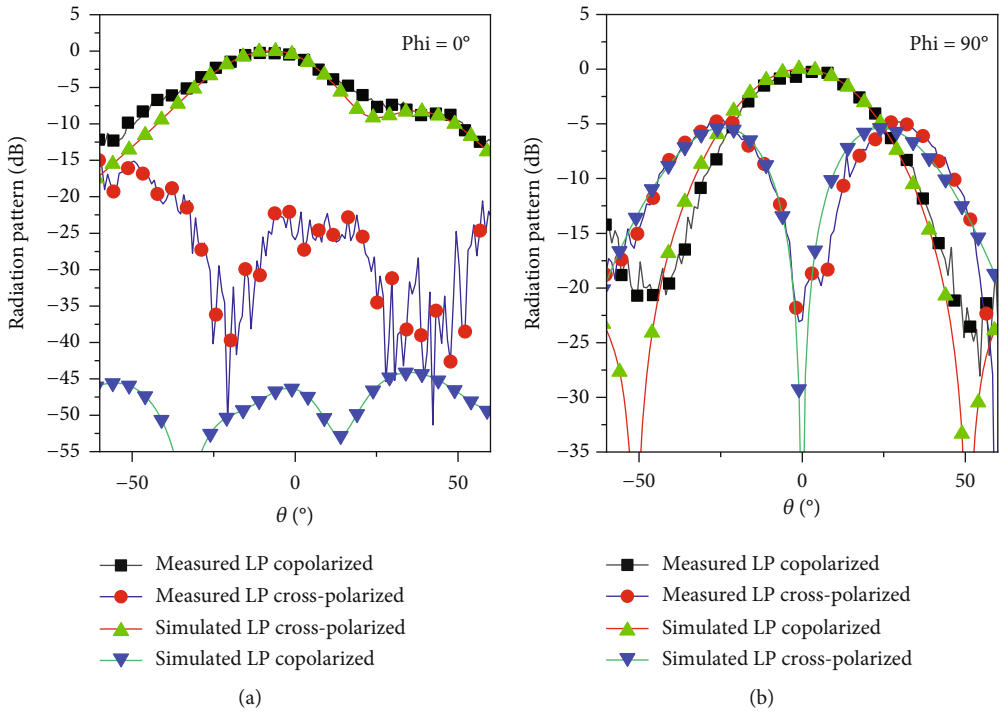

FIGURE 9: The simulated and measured radiation patterns in the $\varphi = 0$ deg and $\varphi = 90$ deg of LP array at 5.3 GHz.

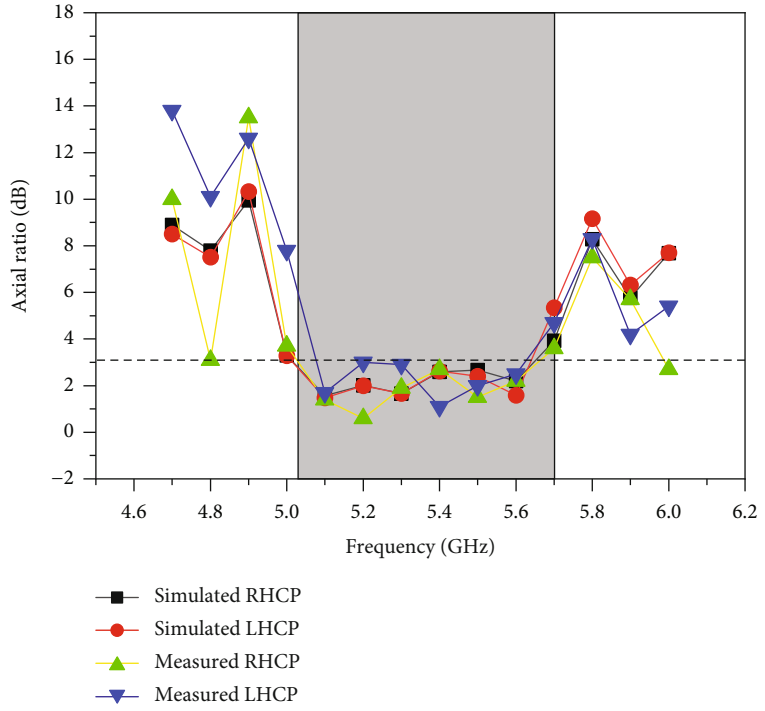

FIGURE 10: Simulated and measured AR.

ARBW of the array is better than that of others, which can meet the requirements of complex communication systems. The polarization of the proposed antenna can be switched. This is the advantage of this antenna array. The isolation between the two ports of the array is lower than −15 dB. The HPBW of the proposed antenna array is wider than the existing work. The realized gain of the antenna is maintained at a normal level.

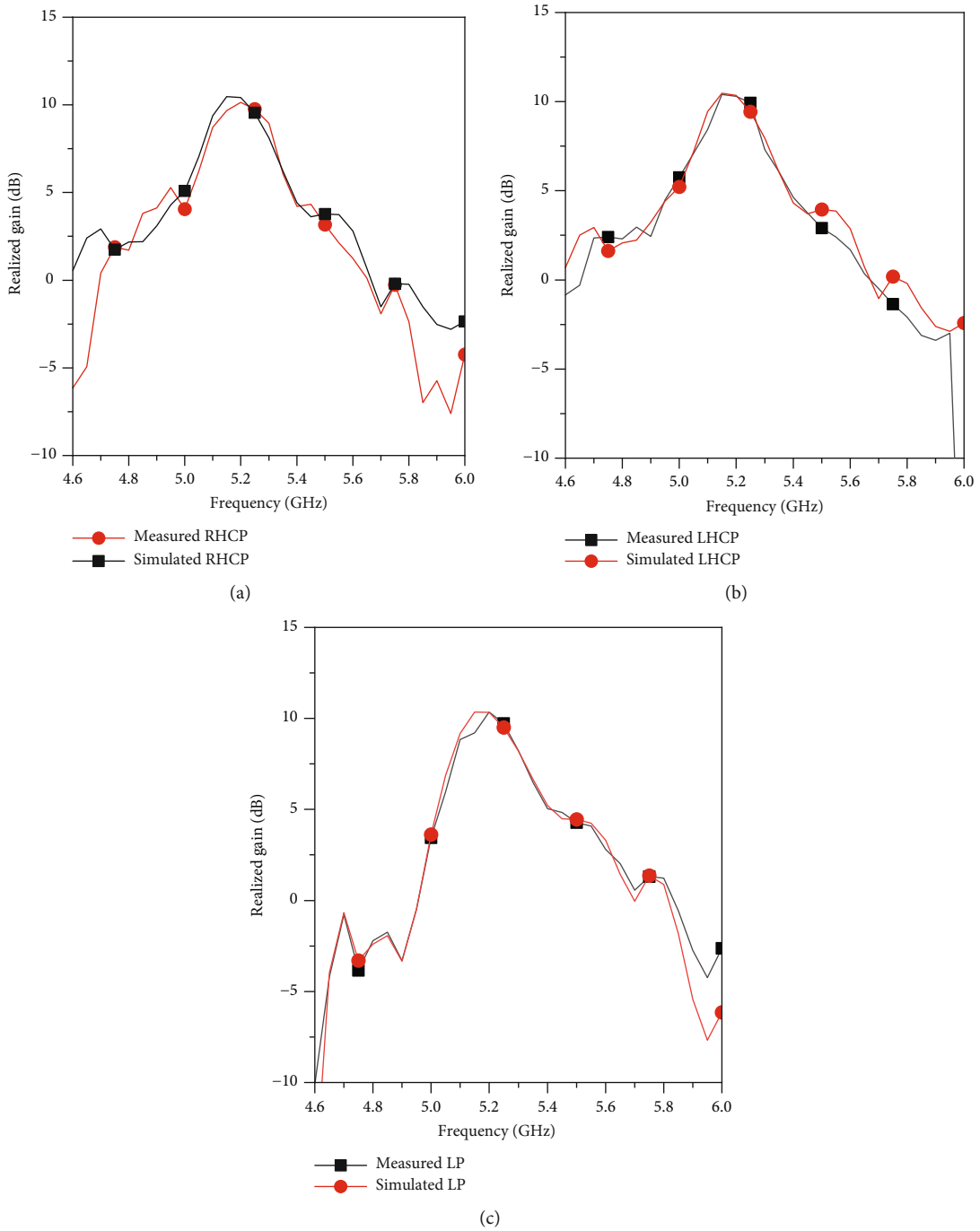

Figure 11: Simulated and measured gain: (a) RHCP, (b) LHCP, and (c) LP.

Table 1: Comparison with the existing antenna work.

Ref.	BW	ARBW	Peak gain (dBic)	Reflection coefficient (dB)	HPBW	Dimension ($\lambda_0 * \lambda_0$)
[5]	63.9%	10%	5.7	-10	NA	1.1 * 1.1
[9]	10.4%	14.5%	24.2	-10	10.8°/12.6°	7 * 7
[14]	6.57%	6.7	11.8	-20	33.5°/35°	3.5 * 2.8
[15]	5.5%	10%	13	-10	35°/32°	2.8 * 2.8
[16]	13.2%	15.7%	11.1	-10	30.5°/35°	3.5 * 2.8
This work	17%	13.2%	10.3	-15	32°/34°	2.3 * 2.3

5. Conclusion

This paper proposed a novel broadband multipolarized traveling-wave series-fed antenna array, which consisted of multiple square unit cells. By adjusting the equivalent length of the unit cell, the bandwidth of the antenna can be increased. The radiation unit cell and dual-port feeding are used in the array, which leads to the possibility of dual circular polarized radiation. Traveling-wave series-fed array can increase bandwidth. Through a reasonable feeding mode, the square unit cell will change between circular polarized (CP) and linear polarized (LP). The isolation between the two ports of the array is lower than −15 dB. The ARBW of the array is 13.2%. The axial ratio in the passband is less than 3 dB. The measured results are consistent with the simulated results. At the same time, the antenna has the function of polarization switching, which can send or receive signals of arbitrary polarization for information matching. This antenna is more suitable for complex communication systems. Polarization conversion of RHCP, LHCP, and LP can be performed at any time.

Data Availability

Data are available on request from the authors.

Conflicts of Interest

The authors declare that they have no conflicts of interest.

Acknowledgments

This works is supported by the National Natural Science Foundations of China (Grant no. 62071040). Help on the measurements is provided by the microwave darkroom of information and communication experimental center of the Beijing University of Technology.

References

[1] K. M. Ibrahim, W. M. Hassan, E. A. Abdallah, and A. M. Attiya, "Wideband sequential feeding network for Ku-band dual circularly polarized 4 × 4 antenna array," *International Journal of RF and Microwave Computer-Aided Engineering*, vol. 30, no. 9, 2020.

[2] M. Fartookzadeh and S. H. Mohseni Armaki, "Serial-feed for a circular patch antenna with circular polarization suitable for arrays," *International Journal of RF and Microwave Computer-Aided Engineering*, vol. 24, no. 5, pp. 529–535, 2014.

[3] Y. X. Guo and D. C. H. Tan, "Wideband single-feed circularly polarized patch antenna with conical radiation pattern," *IEEE Antennas and Wireless Propagation Letters*, vol. 8, pp. 924–926, 2009.

[4] S. X. Ta, H. Choo, I. Park, and R. W. Ziolkowski, "Multi-band, wide-beam, circularly polarized, crossed, asymmetrically barbed dipole antennas for GPS applications," *IEEE Transactions on Antennas and Propagation*, vol. 61, no. 11, pp. 5771–5775, 2013.

[5] Y. Xu, L. Zhu, and N.-W. Liu, "Design approach for a dual-band circularly polarized slot antenna with flexible frequency ratio and similar in-band gain," *IEEE Antennas and Wireless Propagation Letters*, vol. 21, no. 5, pp. 1037–1041, 2022.

[6] O. P. Kumar, T. Ali, and P. Kumar, "A novel corner etched rectangular shaped ultrawideband antenna loaded with truncated ground plane for microwave imaging," *Wireless Personal Communications*, vol. 130, no. 3, pp. 2241–2259, 2023.

[7] O. P. Kumar, T. Ali, P. Kumar, P. Kumar, and J. Anguera, "An elliptical-shaped dual-band UWB notch antenna for wireless applications," *Applied Sciences*, vol. 13, no. 3, p. 1310, 2023.

[8] V. K. Kothapudi and V. Kumar, "SFCFOS uniform and Chebyshev amplitude distribution linear array antenna for K-band applications," *Journal of Electromagnetic Engineering and Science*, vol. 19, no. 1, pp. 64–70, 2019.

[9] V. K. Kothapudi and V. Kumar, "Hybrid-fed shared aperture antenna array for X/K-band airborne synthetic aperture radar applications," *IET Microwaves, Antennas & Propagation*, vol. 15, no. 1, pp. 93–102, 2021.

[10] C. Deng, Y. Li, Z. Zhang, and Z. Feng, "A wideband sequential-phase fed circularly polarized patch array," *IEEE Transactions on Antennas and Propagation*, vol. 62, no. 7, pp. 3890–3893, 2014.

[11] K. H. Lu and T.-N. Chang, "Circularly polarized array antenna with corporate-feed network and series-feed elements," *IEEE Transactions on Antennas and Propagation*, vol. 53, no. 10, pp. 3288–3292, 2005.

[12] M. S. Ellis, Z. Zhao, J. Wu, X. Ding, Z. Nie, and Q.-H. Liu, "A novel simple and compact microstrip-fed circularly polarized wide slot antenna with wide axial ratio bandwidth for C-band applications," *IEEE Transactions on Antennas and Propagation*, vol. 64, no. 4, pp. 1552–1555, 2016.

[13] J. Hu, Z. C. Hao, Z. W. Miao, and Q. Yuan, "Millimeter-wave wideband circularly polarized monopulse antenna using the sequential rotation feeding technique," *International journal of RF and Microwave Computer-Aided Engineering*, vol. 29, no. 1, 2019.

[14] S. J. Chen, C. Fumeaux, Y. Monnai, and W. Withayachumnankul, "Dual circularly polarized series-fed microstrip patch array with coplanar proximity coupling," *IEEE Antennas and Wireless Propagation Letters*, vol. 16, pp. 1500–1503, 2017.

[15] Y. Shen, S.-G. Zhou, G.-L. Huang, and T.-H. Chio, "A compact dual circularly polarized microstrip patch array with interlaced sequentially rotated feed," *IEEE Transactions on Antennas and Propagation*, vol. 64, no. 11, pp. 4933–4936, 2016.

[16] Y.-H. Yang, J.-L. Guo, B.-H. Sun, Y.-M. Cai, and G.-N. Zhou, "The design of dual circularly polarized series-fed arrays," *IEEE Transactions on Antennas and Propagation*, vol. 67, no. 1, pp. 574–579, 2019.

[17] J. Liu and J.-L. Li, "A low-cost, wideband, dual-circularly polarized traveling wave antenna array," *International Journal of RF and Microwave Computer-Aided Engineering*, vol. 31, no. 3, 2021.

[18] Y. Zou, H. Li, Y. Xue, and B. Sun, "A high-gain compact circularly polarized microstrip array antenna with simplified feed network," *International Journal of RF and Microwave Computer-Aided Engineering*, vol. 29, 2019.

[19] X. Guan, Z. Xue, W. Ren, and W. Li, "A multi-polarization series-fed antenna array based on eccentric ring," *IEEE Access*, vol. 11, pp. 23217–23226, 2023.